

# How Does the Critical Point Change during a Chemical Reaction in Supercritical Fluids? A Study of the Hydroformylation of Propene in Supercritical CO<sub>2</sub>

Jie Ke,<sup>†,‡</sup> Buxing Han,<sup>‡</sup> Michael W. George,<sup>†</sup> Haike Yan,<sup>‡</sup> and Martyn Poliakoff<sup>\*,†</sup>

Contribution from the School of Chemistry, University of Nottingham, University Park, Nottingham, NG7 2RD, UK, and Center for Molecular Sciences, Institute of Chemistry, Chinese Academy of Sciences, Beijing 100080, P. R. China

Received September 20, 2000

**Abstract:** An understanding of homogeneous catalysis in supercritical fluids requires a knowledge of the phase behavior and the variation in critical point as the reaction proceeds. In this paper, the critical temperatures,  $T_c$  and pressures,  $P_c$ , have been measured for a considerable number of mixtures representing the various stages of the hydroformylation reaction of propene in supercritical CO<sub>2</sub> and different reactant concentrations. Critical point data have also been measured for all of the binary mixtures of the components (CO<sub>2</sub>, H<sub>2</sub>, CO, propene, *n*- and isobutyraldehyde) which are not available from the literature or can be deduced from published data. We use the stoichiometry of the reacting system to simplify greatly the phase behavior problem by defining a path through the otherwise multidimensional “phase space”. Satisfactory modeling of the data (0.3% in  $T_c$  and 3.0% in  $P_c$ ) has been achieved using the Peng–Robinson equation of state and ignoring all binary interactions which do not involve CO<sub>2</sub>. The model is used to explore the strategies needed to avoid phase separation in continuous and batch reactions. At a given temperature, a batch reactor may need to be run under much higher pressures than a flow reactor if single-phase conditions are to be preserved throughout the course of the reaction. Most of the critical point data were measured acoustically, but a selection of points were validated using more traditional view-cell procedures.

## Introduction

In recent years, increasing numbers of chemists have begun to study reaction chemistry in supercritical fluids (SCFs).<sup>1–4</sup> Some have been attracted by the possibility of environmentally more acceptable replacements for organic solvents,<sup>5</sup> while others have been driven by inherent scientific interest. Whatever their motivation, most workers need to define what is meant by an SCF, and usually they resort to a diagram similar to that in Figure 1. Rarely, do they state that such a diagram only applies to pure substances. Even less frequently is it explained that the phase diagrams for binary mixtures of substances are considerably more complicated<sup>6,7</sup> or that the complexity increases with the number of components in the mixture. However, even the simplest chemical reaction is likely to involve three components (reactant, product, and solvent) and most reactions will involve more. Therefore, any study of reaction chemistry in SCFs necessarily involves the phase equilibrium of multicomponent

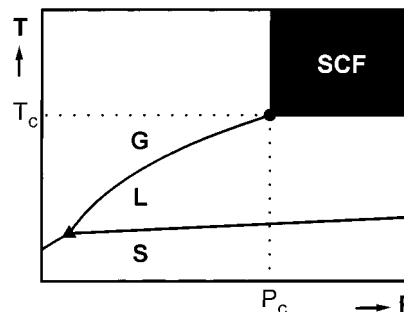


**Figure 1.** Schematic phase diagram of a pure substance: ●, critical point; ▲, triple point; S, solid; L, liquid; G, gas; SCF, supercritical fluid. Such diagrams are usually presented with the  $T$  and  $P$  axes reversed. We believe that the orientation shown here is probably more effective for teaching purposes.

mixtures. This phase behavior is important because the outcome reaction can sometimes be determined by whether the reaction mixture is single- or multiphase.

The study of phase equilibrium is a long established field,<sup>8–13</sup> although most studies are restricted to mixtures with relatively small number of components. Reaction mixtures differ from

\* To whom correspondence should be addressed. <http://www.nottingham.ac.uk/supercritical/>.

<sup>†</sup> The School of Chemistry.

<sup>‡</sup> Center for Molecular Sciences.

(1) Jessop, P. G.; *Top. Catal.* **1998**, *5*, 95–103.

(2) Jessop, P. G.; Ikariya, T.; Noyori, R. *Chem. Rev.* **1999**, *99*, 475–493.

(3) *Chemical Synthesis Using Supercritical Fluids*; Jessop, P. G., Leitner, W., Eds.; Wiley–VCH: Weinheim, 1999.

(4) Darr, J. A.; Poliakoff, M. *Chem. Rev.* **1999**, *99*, 495–541.

(5) *Green Chemistry: Frontiers in Benign Chemical Synthesis*; Anastas, P. T., Williamson, T. C., Eds.; Oxford University Press: Oxford, 1998.

(6) Van Konynenburg, P. H.; Scott, R. L. *Philos. Trans. R. Soc. London, Ser. A* **1980**, *298*, 495–540.

(7) McHugh, M. A.; Krukonis, V. J. *Supercritical Fluid Extraction*, 2nd ed.; Butterworth-Heinemann: Boston, 1994.

(8) Hicks, C. P.; Young, C. L. *Chem. Rev.* **1975**, *75*, 119–175.

(9) Schneider, G. M. In *A Specialist Periodical Report*; McGlashan, M. L., Ed.; Chemical Thermodynamics, Vol 2; The Chemical Society: London, 1978; pp 105–146.

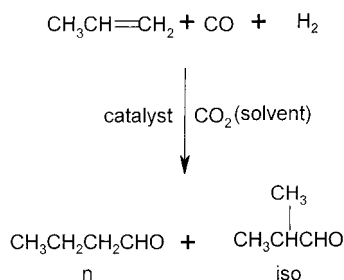
(10) Rowlinson, J. S.; Swinton, F. L. *Liquids and Liquid Mixtures*, 3rd ed.; Butterworth: London, 1982.

(11) Schneider, G. M. *Pure Appl. Chem.* **1983**, *55*, 479–492.

(12) McGlashan, M. L. *Pure Appl. Chem.* **1985**, *57*, 89–103.

(13) Sadus, R. J. *AIChE J.* **1994**, *40*, 1376–1403.

## Scheme 1



those which are normally studied because, by definition, their chemical composition changes with time. Hence, the critical points of reaction mixtures will also change with time.

A number of recent studies have begun to address phase equilibria of reaction mixtures. Brennecke and co-workers<sup>14</sup> presented an elegant study of binary mixtures (CO<sub>2</sub> + reactants, CO<sub>2</sub> + products, etc.) and used these results to model the phase equilibrium, but not the critical points, of a catalytic epoxidation reaction. A series of three papers<sup>15–17</sup> from Chrisochoou, Stephan, and co-workers has described the phase equilibrium but not the critical points of mixtures containing up to five components, involved in an enzymatic reaction in scCO<sub>2</sub>. However, critical points are important because it is here that nonideal behavior is greatest and models are most likely to fail.<sup>18</sup> In this paper, we present the first study aimed at answering the question “How does the critical point change during a chemical reaction in an SCF?” This question is important because, in many cases, it may be crucial to keep the reaction mixture as a single phase throughout the reaction.

We have based our study upon a test reaction, the hydroformylation of propene (C<sub>3</sub>H<sub>6</sub>) in scCO<sub>2</sub>, see Scheme 1.

This reaction has been chosen for a number of reasons: (1) there is considerable current interest in hydroformylation in SCF,<sup>19–37</sup> (2) the reaction of C<sub>3</sub>H<sub>6</sub> has been particularly well-studied by a number of groups,<sup>19–21,38</sup> and (3) the reaction involves six species, H<sub>2</sub>, CO, CO<sub>2</sub>, C<sub>3</sub>H<sub>6</sub>, *n*-butyraldehyde, isobutyraldehyde which span a wide range of critical parameters. These components give rise to 15 possible binary mixtures. Our

strategy has been to measure the critical curves of all binary mixtures involving CO<sub>2</sub>, and of a series of three, four, and six components to provide enough data to test the modeling of the reaction. We use the stoichiometry of the reaction to simplify the problem by defining a relatively precise path through the multidimensional space associated with a six-component mixture. This simplification allows us to discuss the best strategy for maintaining the mixtures in a single phase throughout the reaction. The strategies turn out to be different for continuous and batch reactors.

Our measurement of critical points is based on an acoustic technique, which has been described in some detail previously.<sup>39–43</sup> This technique is relatively fast compared to other phase equilibrium measurements, thus allowing us to measure the critical points of several hundred samples for the study reported here. The basis of the technique is that the velocity of sound reaches a minimum at the critical point of a pure substance, and very close to the critical point for a wide range of mixtures. The advantage, compared to a view-cell, is that acoustics give an indication of the critical density even at temperatures significantly above the critical temperature,<sup>41,43</sup> *T*<sub>c</sub>, hence accelerating the location of *T*<sub>c</sub> itself. The acoustic technique does not necessarily work with all mixtures. Therefore we have validated our measurements by confirming the critical points of key mixtures by using a more conventional variable-volume view-cell.

In what follows, we describe our experimental technique and present data for a series of binary and more complicated mixtures. We then use these data to develop and test a relatively simple but surprisingly effective model based on the Peng–Robinson equation of state (PR EOS) to describe the systems. Overall, we show that the behavior of such a reaction system is simpler than anticipated and, therefore, is much more amenable to detailed analysis than was previously supposed. We then use these results to define the best conditions for running the reaction both as batch and continuous processes.

## Experimental Section

**Apparatus and the Method of Preparing Samples.** The measurements were made using an acoustic technique, which can be regarded as a nonvisual synthetic method.<sup>44</sup> The phase transition of a sample with a constant overall composition can be detected by changes in the velocity of sound. The apparatus and the experimental procedure used

(14) Stradi, B. A.; Kohn, J. P.; Stadtherr, M. A.; Brennecke, J. F. *J. Supercrit. Fluids* **1998**, *12*, 109–122; the same group has recently published a reliable method for computing the critical points of mixtures (Stradi, B. A.; Brennecke, J. F.; Kohn, J. P.; Stadtherr, M. A., *AIChE J.* **2001**, *47*, 212–221).

(15) Chrisochoou, A.; Schaber, K.; Bolz, U. *Fluid Phase Equilib.* **1995**, *108*, 1–14.

(16) Chrisochoou, A. A.; Schaber, K.; Stephan, K. *J. Chem. Eng. Data* **1997**, *42*, 551–557.

(17) Chrisochoou, A. A.; Schaber, K.; Stephan, K. *J. Chem. Eng. Data* **1997**, *42*, 558–561.

(18) Levelt Sengers, J. M. H. In *Supercritical Fluids: Fundamentals for Application*; Kiran, E., Levelt Sengers, J. M. H., Eds.; Kluwer: Dordrecht, The Netherlands, 1994.

(19) Rathke, J. W.; Klingler, R. J.; Krause, T. R. *Organometallics* **1991**, *10*, 1350.

(20) Abraham, M.; Snyder, G. *Abs. Papers Am. Chem. Soc.* **1999**, *218*, 80-IEC.

(21) Abraham, M. A.; Snyder, G. In *5th International Symp. on Supercritical Fluids*; Atlanta, 2000; p 7.

(22) Bach, I.; Cole-Hamilton, D. J. *Chem. Commun.* **1998**, 1463–1464.

(23) Bischoff, S.; Kant, M. *Ind. Eng. Chem. Res.* **2000**, *39*, 4908–4913.

(24) Cole-Hamilton, D. J.; Sellin, M. F. *Abs. Papers Am. Chem. Soc.* **1999**, *218*, 344-INOR.

(25) Davis, T.; Erkey, C. *Ind. Eng. Chem. Res.* **2000**, *39*, 3671–3678.

(26) Dharmadhikari, S.; Abraham, M. A. *J. Supercrit. Fluids* **2000**, *18*, 1–10.

(27) Francio, G.; Leitner, W. *Chem. Commun.* **1999**, 1663–1664.

(28) Kainz, S.; Leitner, W. *Catal. Lett.* **1998**, *55*, 223–225.

(29) Kainz, S.; Koch, D.; Baumann, W.; Leitner, W. *Angew. Chem., Int. Ed. Engl.* **1997**, *36*, 1628–1630.

(30) Koch, D.; Leitner, W. *J. Am. Chem. Soc.* **1998**, *120*, 13398–13404.

(31) Kramarz, K. W.; Klingler, R. J.; Fremgen, D. E.; Rathke, J. W. *Catal. Today* **1999**, *49*, 339–352.

(32) Meehan, N. J.; Sandee, A. J.; Reek, J. N. H.; Kamer, P. J. C.; van Leeuwen, P. W. M. N.; Poliakov, M. *Chem. Commun.* **2000**, 1497–1498.

(33) Palo, D. R.; Erkey, C. *Ind. Eng. Chem. Res.* **1998**, *37*, 4203–4206.

(34) Palo, D. R.; Erkey, C. *Ind. Eng. Chem. Res.* **1999**, *38*, 3786–3792.

(35) Palo, D. R.; Erkey, C. *Ind. Eng. Chem. Res.* **1999**, *38*, 2163–2165.

(36) Palo, D. R.; Erkey, C. *Organometallics* **2000**, *19*, 81–86.

(37) Osuna, A. M. B.; Chen, W. P.; Hope, E. G.; Kemmitt, R. D. W.; Paige, D. R.; Stuart, A. M.; Xiao, J. L.; Xu, L. J. *J. Chem. Soc., Dalton Trans.* **2000**, 4052–4055.

(38) Guo, Y.; Akgerman, A. *Ind. Eng. Chem. Res.* **1997**, *36*, 4581–4585.

(39) Kordikowski, A.; Robertson, D. G.; Aguiar-Ricardo, A. I.; Popov, V. K.; Howdle, S. M.; Poliakov, M. *J. Phys. Chem.* **1996**, *100*, 9522–9526.

(40) Kordikowski, A.; Robertson, D. G.; Poliakov, M.; Di Noia, T. D.; McHugh, M.; Aguiar-Ricardo, A. *J. Phys. Chem. B* **1997**, *101*, 5853–5862.

(41) Kordikowski, A.; Poliakov, M. *Fluid Phase Equilib.* **1998**, *151*, 493–499.

(42) Popov, V. K.; Banister, J. A.; Bagratashvili, V. N.; Howdle, S. M.; Poliakov, M. *J. Supercrit. Fluids* **1994**, *7*, 69–73.

(43) Ke, J.; Han, B.; George, M. W.; Yan, H.; Poliakov, M. In *14th Symposium on Thermophysical Properties*; Haynes, W. M., Stevenson, B. A., Eds.; Boulder, Colorado, U.S.A., 2000.

(44) Dohrn, D.; Brunner, G. *Fluid Phase Equilib.* **1995**, *106*, 213–282.

in this work have been described in detail by Kordikowski et al.<sup>39,40</sup> The apparatus consists of an acoustic cavity, in which two identical ceramic transducers are mounted, facing each other. An acoustic signal is provided by a pulse generator (1  $\mu$ s wide pulses at a repetition rate of  $\sim$ 100 Hz). The resulting signal is amplified and displayed on an oscilloscope, from which the transit time of the pulse travelling between the transducers is obtained. A manual high-pressure pump is used to adjust the system pressure to the desired value within  $\pm$ 0.1 bar. The acoustic cavity is mounted in an insulated aluminum jacket, the temperature of which is controlled to within  $\pm$ 0.1 K by a circulating water/glycol thermostat. The pump and acoustic cavity are held at the same temperature.

Samples of multicomponent mixtures were prepared as follows. Initially, the apparatus was evacuated and flushed with CO<sub>2</sub>. A measured weight of the heavy component (e.g., butyraldehyde) was added as a liquid to the cell by syringe. Then, gases, such as C<sub>3</sub>H<sub>6</sub>, CO, and H<sub>2</sub> were added from high-pressure reservoirs. The amount of gas was calculated from the pressure, temperature, and total volume of the system. The cell and pump were kept at a constant, known temperature during this process. Finally, CO<sub>2</sub> was expanded into the system from a high-pressure bomb. The weight difference of the bomb was used to determine the amount of CO<sub>2</sub> which had been added. The fluid was repeatedly compressed and expanded inside the cell and the pump for at least 6 h to ensure adequate mixing of the sample. The temperature and pressure of the system were kept high enough to ensure that no phase separation occurred. Before the measurement was started, the apparatus was allowed to equilibrate for 30 min at the desired temperature. The acoustic time delay was measured as a function of pressure along each isotherm. The mixing procedure was then repeated to guarantee that a homogeneous liquid phase was present prior to any experiments. The error in the composition of C<sub>3</sub>H<sub>6</sub>/CO/H<sub>2</sub> mixture is essentially due to pressure measurements, that is,  $\sim$  $\pm$ 0.1 bar. The error in the gravimetric measurements was  $\pm$ 0.1 mg for butyraldehydes and  $\pm$ 10 mg for CO<sub>2</sub>. Hence, it is possible to set the conversion, which depends on the mole ratio of butyraldehydes and C<sub>3</sub>H<sub>6</sub>/CO/H<sub>2</sub>, to a desired value within  $\pm$ 1%.

**Validation with a View-Cell.** To validate the critical points measured using the acoustic method, some measurements were repeated visually. A variable volume cell<sup>45</sup> with two borosilicate glass windows was assembled. The cell was placed in a water bath, the temperature of which was maintained with a heater/circulator to  $\pm$ 0.2 K. A magnetic stirrer was used to ensure that the contents of the cell were well mixed. Samples were prepared using the same method, as described above, for samples in the acoustic experiments. The overall error was  $\pm$ 0.2 K for  $T_c$  and  $\pm$ 0.3 bar for  $P_c$ , respectively. A detailed description of the apparatus and procedures can be found elsewhere.<sup>45</sup> Separate samples of the same nominal composition were made up for acoustic and visual experiments. Some additional errors may have been introduced by small differences in the ratio of the solutes (e.g., C<sub>3</sub>H<sub>6</sub>, CO, H<sub>2</sub>, and two butyraldehydes) between the acoustic and visual samples.

**Materials.** Carbon monoxide (Air Products, purity 99.8%), propene, carbon dioxide, and hydrogen (BOC, purities of 99.8, 99.99, and 99.995%, respectively) and *n*-butyraldehyde and isobutyraldehyde (Aldrich, purity stated higher than 99.5 and 99%, respectively) were used as supplied.

## Results and Discussion

**Critical Points of the Reaction Mixture (Six-Component System).** The reaction mixture for hydroformylation of propene consists of three reactants (C<sub>3</sub>H<sub>6</sub>, CO, and H<sub>2</sub>), two products (*n*- and isobutyraldehyde), and the solvent (CO<sub>2</sub>), as shown in Scheme 1. Strictly, the catalyst is a seventh component, but we have ignored it in our discussions here, because its concentration is low and sometimes a heterogeneous catalyst is used.<sup>32</sup> Five independent mole fractions are necessary to describe the composition in a six-component mixture. Clearly, the phase behavior of such mixtures is potentially quite complex. To

**Table 1.** Critical Points<sup>a</sup> of CO<sub>2</sub> + *n*-butyraldehyde<sup>b</sup> + isobutyraldehyde<sup>b</sup> + C<sub>3</sub>H<sub>6</sub><sup>c</sup> + CO<sup>c</sup> + H<sub>2</sub><sup>c</sup> Mixtures

$\chi_0^d$	$T_c$ /K	$P_c$ /bar	$\chi_0^d$	$T_c$ /K	$P_c$ /bar
	$\alpha = 0^e$			$\alpha = 0.75^e$	
0.060	302.6	82.3	0.054	311.1	82.0
0.12	300.8	89.3	0.11	314.6	88.3
0.18	298.5	95.8	0.16	323.0	98.8
0.25	297.0	105.1	0.22	328.5	108.0
	$\alpha = 0.30^e$			$\alpha = 1.00^{e,f}$	
0.067	307.0	85.3	0.052	312.8	81.2
0.10	307.8	90.0	0.092	320.1	88.1
0.14	308.6	97.0	0.15	329.7	96.0
0.21	310.3	106.7	0.24	338.4	104.5
	$\alpha = 0.49^e$				
0.064	309.3	84.7			
0.11	311.9	92.7			
0.16	315.3	100.7			
0.29	320.2	118.4			

<sup>a</sup> Error of  $T_c$  and  $P_c$  are  $\pm$ 0.3 K and  $\pm$ 0.4 bar, respectively. <sup>b</sup> The molar ratio of *n*-butyraldehyde to isobutyraldehyde is 8:1. <sup>c</sup> The molar ratio C<sub>3</sub>H<sub>6</sub>:CO:H<sub>2</sub> is 1:1:1. <sup>d</sup>  $\chi_0$  represents the initial total mole fraction of the reactants when there are no products. <sup>e</sup>  $\alpha$  is conversion,  $\alpha = (\text{the moles of the reactants reacted})/(\text{initial moles of the reactants})$ .<sup>f</sup> When  $\alpha = 1$ , all reactants have been consumed, and the mixture contains only CO<sub>2</sub> + aldehydes.

simplify the problem, the multicomponent mixture can be investigated just at certain fixed compositions. In this work, we have fixed the molar ratio C<sub>3</sub>H<sub>6</sub>:CO:H<sub>2</sub> at 1:1:1 (the stoichiometric amount)<sup>46</sup> and the molar ratio of *n*-butyraldehyde to isobutyraldehyde at 8:1 (the experimental value<sup>19,47</sup>). Then, we introduce two variables,  $\chi_0$  and  $\alpha$ , to simulate the reaction process.  $\chi_0$  is the initial total mole fraction of the reactants at the start of the reaction.  $\alpha$  is the conversion, which we define as the fraction of reactants that have been converted to products at a given stage of the reaction.<sup>48</sup> Thus,  $\alpha = 0$  at the start, 1 at the finish, and 0.5 at the exact midpoint of the reaction (i.e., when 50% of the reactants have been converted). Given the stoichiometric relation between products and reactants, the mole fractions of all six components can be represented merely in terms of  $\chi_0$  and  $\alpha$ .

$T_c$  and  $P_c$  were measured for mixtures corresponding to five conversions: 0, 0.30, 0.49, 0.75, and 1.00. The initial total mole fractions,  $\chi_0$ , ranged from 0 to 0.29. The results are summarized in Table 1, and three projections,  $P-\chi_0$ ,  $T-\chi_0$ , and  $P-T$ , of the critical points are shown in Figure 2. At  $\alpha = 0$ , there is a quaternary mixture (CO<sub>2</sub> + C<sub>3</sub>H<sub>6</sub> + CO + H<sub>2</sub>). Since CO and H<sub>2</sub> are permanent gases with very low critical temperatures, it is not surprising that  $T_c$  decreases for increasing amounts of CO and H<sub>2</sub> in the mixture. Thus, it can be seen from Figure 2c that  $T_c$  decreases with increasing  $\chi_0$  for  $\alpha = 0$ . As  $\alpha$  increases, the mixture contains more butyraldehydes, and the mole fractions of CO and H<sub>2</sub> decrease. If  $\alpha$  is large enough, the effect of the butyraldehydes on  $T_c$  is dominant. Since the critical temperatures of two butyraldehydes are much higher than that of CO<sub>2</sub> (see Table 4),  $T_c$  of the reaction mixture increases with  $\chi_0$  at conversions of 0.30, 0.49, 0.75, and 1.00 (Figure 2c). Figure 2a shows that  $P_c$  for mixtures with the same conversion start from  $P_c$  of pure CO<sub>2</sub> and extend to high pressure. No

(46) In actual reactions an excess of syngas (CO + H<sub>2</sub>) would be used, but this would not change the overall conclusions of our experiments.

(47) Other catalysts may well give different *n*:*iso* ratios but this would not affect the overall conclusions of our study.

(48) It has been pointed out (Schneider, G. M., private communication.) that this approach is in fact an extension of Denbigh's treatment of the Phase Rule as applied to stoichiometric mixtures in equilibrium (Denbigh, K. *The Principles of Chemical Equilibrium*, 4th ed.; Cambridge University Press: Cambridge, 1981; p 190).

(45) Zhang, H.; Han, B.; Hou, Z.; Liu, Z. In *Proceedings of the 5th International Symposium on Supercritical Fluids*: Atlanta, GA, U.S.A., 2000.



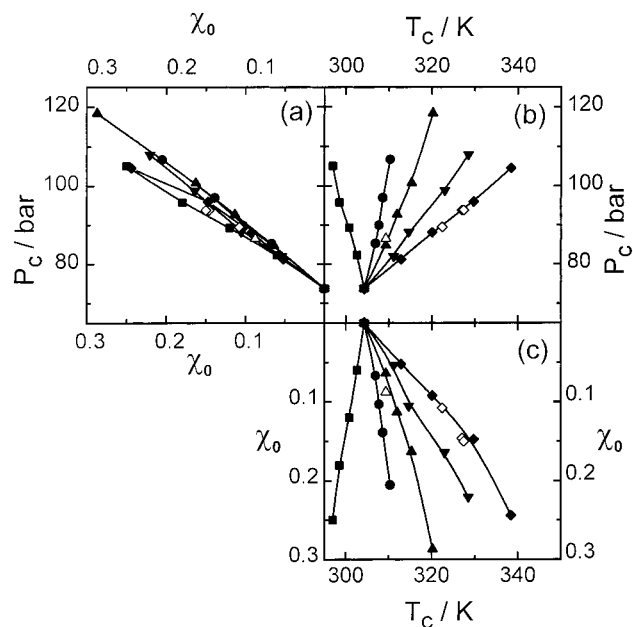


**Figure 2.** The critical points of the reaction mixture for hydroformylation of  $C_3H_6$ : (a)  $P$ - $\chi_0$  projection, (b)  $P$ - $T$  projection, (c)  $T$ - $\chi_0$  projection.  $\blacksquare$ ,  $\alpha = 0$ ;  $\bullet$ ,  $\alpha = 0.30$ ;  $\blacktriangle$ ,  $\alpha = 0.49$ ;  $\blacktriangledown$ ,  $\alpha = 0.75$ ;  $\blacklozenge$ ,  $\alpha = 1.00$ ; —, curves fitted to acoustic data. Open points are measurements made visually with a view-cell. It can be seen that the agreement between acoustic and visual methods is good.  $\triangle$ ,  $\alpha = 0.49$ ;  $\diamond$ ,  $\alpha = 1.00$ .

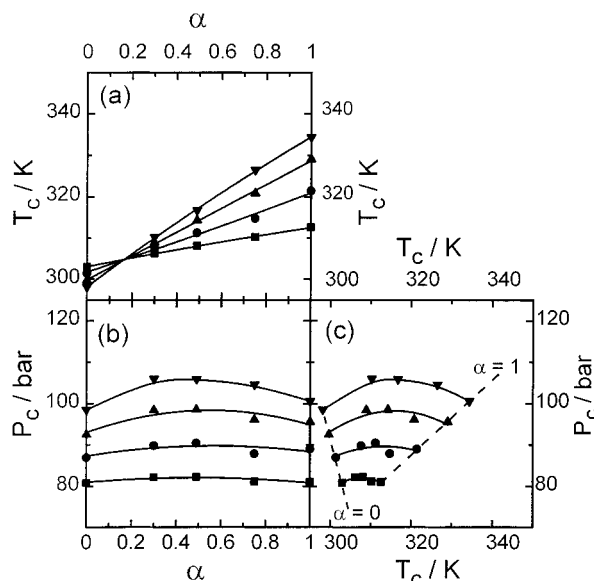


**Figure 3.** The critical points of the reaction mixture for hydroformylation of  $C_3H_6$ : (a)  $T$ - $\alpha$  projection, (b)  $P$ - $\alpha$  projection, (c)  $P$ - $T$  projection.  $\blacksquare$ ,  $\chi_0 = 0.05$ ;  $\bullet$ ,  $\chi_0 = 0.10$ ;  $\blacktriangle$ ,  $\chi_0 = 0.15$ ;  $\blacktriangledown$ ,  $\chi_0 = 0.20$ ; —, curves fitted to experimental data. The data in this Figure are smoothed values taken from Table 1.

pressure maximum was found because only mixtures with the initial total mole fraction up to 0.29 were measured. The  $P$ - $T$  projection is given in Figure 2b. The critical curves for mixtures with the same conversion are almost straight lines radiating from the critical point of pure  $CO_2$ . At  $\alpha = 0$ , the critical curve shows a negative slope, while the curves with  $\alpha > 0.30$  exhibit a positive slope.

Figure 3 illustrates the dependence of the  $T_c$  and  $P_c$  on  $\alpha$  for different values of  $\chi_0$ . How far  $T_c$  of the reaction mixtures differs from that of pure  $CO_2$  depends on both  $\alpha$  and  $\chi_0$ . For a given  $\chi_0$ ,  $T_c$  increases for increasing  $\alpha$  (Figure 3a), and a crossover

**Table 2.** Experimental Critical Points<sup>a</sup> for Binary Systems Containing  $CO_2$

$x_2^b$	$T_c/K$	$P_c/\text{bar}$	$x_2^b$	$T_c/K$	$P_c/\text{bar}$
$CO_2(1) + n\text{-butyraldehyde}(2)$			$CO_2(1) + CO(2)$		
0.019	313.8	82.5	0.070	298.2	81.0
0.031	318.9	86.9	0.122	292.5	88.1
0.057	330.0	96.9	0.159	289.0	92.6
0.076	333.0	99.9	0.227	283.5	96.8
0.079	333.7	100.5	0.271	280.2	99.2
0.100	337.6	103.6			
$CO_2(1) + \textit{i}\text{-butyraldehyde}(2)$			$CO_2(1) + H_2(2)$		
0.014	311.5	80.9	0.043	303.7	91.6
0.035	320.0	88.5	0.106	300.3	116.4
0.042	323.3	91.6	0.114	300.0	117.7
0.051	327.0	94.0	0.148	298.0	131.5
0.071	330.5	97.4	0.168	297.6	134.7
			0.201	296.7	138.3
$CO_2(1) + C_3H_6(2)^c$					
0.051	305.4	71.8			
0.109	308.0	70.2			
0.233	313.8	68.6			
0.384	325.0	66.5			
0.468	329.3	65.8			
0.623	343.8	60.0			

<sup>a</sup> Error of  $T_c$  and  $P_c$  are  $\pm 0.3$  K and  $\pm 0.4$  bar, respectively. <sup>b</sup> Mole fraction of component 2. <sup>c</sup> Measured by the visual method; error of  $T_c$  and  $P_c$  are  $\pm 0.2$  K and  $\pm 0.3$  bar, respectively.

point is observed at  $\alpha = 0.14$ , where  $T_c$  is 304 K, the same as that of pure  $CO_2$ . This means that  $T_c$ , the critical temperature, for  $\alpha = 0.14$  is independent of  $\chi_0$ , at least up to  $\chi_0 = 0.20$ . As mentioned previously, the addition of reactants decreases the overall value of  $T_c$ , whereas the products have the opposite effect on  $T_c$  of the mixture. When  $\alpha = 0.14$ , the two effects canceled out, even when  $\chi_0$  is varied over a significant range. It should be noted that, even at  $\alpha = 0.14$ ,  $P_c$ , the critical pressure, increases with the increasing of  $\chi_0$ , as shown in Figure 3b. Furthermore, a slight maximum for  $P_c$  is observed as  $\alpha$  increases, especially for the mixtures with high  $\chi_0$ . It can be seen from Figure 3b that the maximum critical pressure is located at  $\alpha = 0.30$ .

Figure 3c is a particularly important diagram. It shows how the critical point changes in the course of the reaction as  $\chi_0$  increases (i.e. for increasingly concentrated reaction mixtures). However, as explained later, a more comprehensive diagram is needed to decide whether a particular mixture will remain in a single phase throughout the whole reaction.

**Critical Points of the Binary Mixtures Containing  $CO_2$ .** Four binary systems  $CO_2 + n$ -butyraldehyde,  $CO_2 + \textit{i}\text{-butyraldehyde}$ ,  $CO_2 + CO$ , and  $CO_2 + H_2$  were measured with our acoustic apparatus. The results are given in Table 2.

The binary system  $CO_2 + n$ -butyraldehyde was studied at six different compositions, and five mixtures were investigated for the system  $CO_2 + \textit{i}\text{-butyraldehyde}$ . The compositions of the butyraldehyde mixtures correspond to those in the six-component reaction mixtures. The  $P$ - $x$ ,  $T$ - $x$  and  $P$ - $T$  projections of these two systems are shown in Figure 4. The critical curves are almost straight lines in the  $CO_2$ -rich region (Figure 4b). Also the two curves are nearly coincident over the temperature range, 305–325 K. This suggests that for the ternary mixture  $CO_2 + n$ - +  $\textit{i}\text{-butyraldehyde}$ , the critical points would not change significantly in the  $CO_2$ -rich region if the molar ratio of  $n$ -butyraldehyde to  $\textit{i}\text{-butyraldehyde}$  were varied. However, in much more concentrated binary mixtures, larger differences between two critical curves are likely to be observed because the differences in  $T_c$  and  $P_c$  between the two butyraldehydes are 32.4 K and 12.3 bar, respectively.

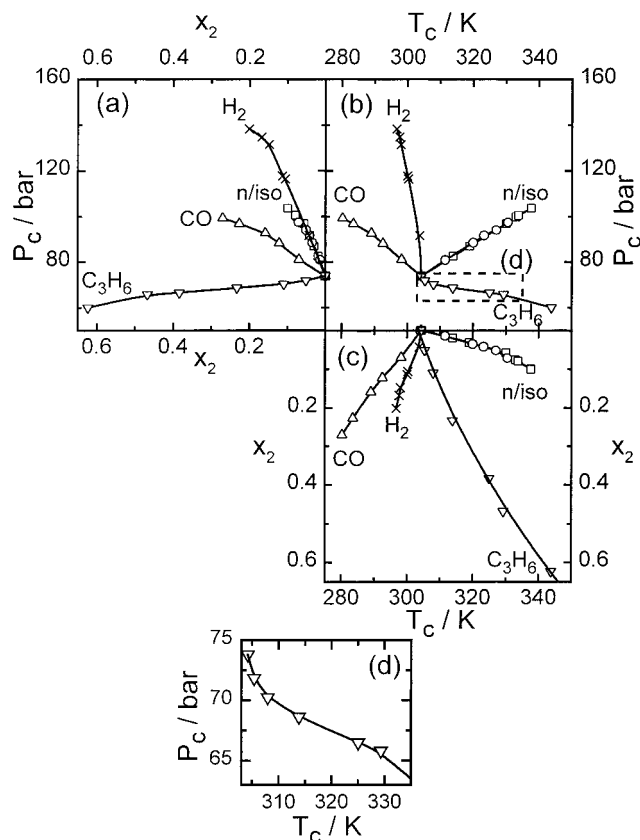


**Figure 4.** The critical points of binary systems containing CO<sub>2</sub>: (a)  $P$ - $x$  projection, (b)  $P$ - $T$  projection, (c)  $T$ - $x$  projection, (d) enlarged portion of the line for CO<sub>2</sub> + C<sub>3</sub>H<sub>6</sub> in the  $P$ - $T$  projection, illustrating the point of inflection. □, (CO<sub>2</sub> + *n*-butylaldehyde); ○, (CO<sub>2</sub> + isobutylaldehyde); ▽, (CO<sub>2</sub> + C<sub>3</sub>H<sub>6</sub>); △, (CO<sub>2</sub> + CO); ×, (CO<sub>2</sub> + H<sub>2</sub>); —, curves fitted to experimental data.

The vapor-liquid equilibrium of the system CO<sub>2</sub> + H<sub>2</sub> has been measured by Tsang and Streett<sup>49</sup> at temperature from 220 to 290 K. The critical points were interpolated by these authors from their  $P$ - $T$ - $x$  data, covering compositions from 0.2675 to 0.64 (mole fraction of H<sub>2</sub>). According to their study, the CO<sub>2</sub> + H<sub>2</sub> system shows type-III phase behavior in the Scott and Konynenburg classification.<sup>6</sup> This implies that there is no continuous critical locus at low temperatures. Our measurements determined the critical point directly for mole fractions of H<sub>2</sub> < 0.21 (i.e. at lower concentrations of H<sub>2</sub> than used by Tsang and Streett). We found that  $T_c$  decreased slightly, but  $P_c$  increased dramatically with the addition of H<sub>2</sub> (Figure 4). These results confirm our previous finding that  $P_c$  can be used to quantify small amounts of permanent gases, such as He, H<sub>2</sub>, and N<sub>2</sub>, in CO<sub>2</sub>.<sup>42,50</sup> The critical line for the binary system CO<sub>2</sub> + CO is also shown in Figure 4. Five different mixtures were investigated with the mole fraction of CO < 0.28. The critical curve starts from the critical point of CO<sub>2</sub> and extends to low temperature. In contrast to CO<sub>2</sub> + H<sub>2</sub>,  $T_c$  of the CO<sub>2</sub> + CO mixture decreases substantially with increasing amounts of CO. Since the triple point temperature of CO<sub>2</sub> (216.58 K) is much higher than the critical temperature of CO (132.95 K), no continuous critical line between two critical points are expected for this system.

The system CO<sub>2</sub> + C<sub>3</sub>H<sub>6</sub> has been extensively studied,<sup>51-55</sup> but most measurements have not focused on critical points. We

(49) Tsang, C. Y.; Streett, W. B. *Chem. Eng. Sci.* **1981**, *36*, 993-1000.

(50) Kordikowski, A.; Robertson, D. G.; Poliakoff, M. *Anal. Chem.* **1996**, *68*, 4436-4440.

(51) Winkler, C. A.; Maass, O. *Can. J. Res.* **1932**, *6*, 458-470.

**Table 3.** Critical Points<sup>a</sup> for the Ternary System of CO<sub>2</sub> + CO + H<sub>2</sub>

$x_{\text{CO}}$	$x_{\text{H}_2}$	$T_c/\text{K}$	$P_c/\text{bar}$
$x_{\text{CO}}:x_{\text{H}_2} = 2:1$			
0.036	0.018	300.6	83.7
0.071	0.035	296.1	94.1
0.129	0.064	288.6	110.6
0.158	0.079	284.7	121.5
0.193	0.097	281.5	126.1
$x_{\text{CO}}:x_{\text{H}_2} = 1:1$			
0.023	0.023	302.4	85.1
0.053	0.053	297.5	97.6
0.078	0.078	293.6	111.0
0.105	0.105	290.1	122.1
0.145	0.145	286.5	128.7
$x_{\text{CO}}:x_{\text{H}_2} = 1:2$			
0.014	0.027	302.7	85.7
0.038	0.076	297.7	105.9
0.054	0.107	293.9	122.8
0.066	0.131	291.9	131.8
0.089	0.177	289.5	137.5

<sup>a</sup> Error of  $T_c$  and  $P_c$  are  $\pm 0.3$  K and  $\pm 0.4$  bar, respectively.

report six new critical points, all obtained visually (see Table 2). The system exhibits type-I fluid-phase behavior, which means that a continuous critical line connects the critical points of the two pure components. It can be seen from Figure 4 that  $T_c$  increases with the increasing of  $x_{\text{C}_3\text{H}_6}$ , but  $P_c$  decreases with  $x_{\text{C}_3\text{H}_6}$ . Also a point of inflection is observed in the  $P$ - $T$  projection (see Figure 4d).

**Ternary System (CO<sub>2</sub> + CO + H<sub>2</sub>).** Previously, this ternary system has only been studied at temperatures well below  $T_c$ .<sup>56</sup> Here, the critical points have been measured for three fixed CO:H<sub>2</sub> molar ratios, 2:1, 1:1, and 1:2. The critical points are listed in Table 3. Because our primary goal was to construct the critical surface in the CO<sub>2</sub>-rich region, five mixtures at each molar ratio were studied with the mole fraction of CO<sub>2</sub> varying between 0.71 and 0.96. Figure 5 shows the three projections of the ternary critical points. The ternary critical points for mixtures with the same ratio of CO to H<sub>2</sub> all lie on a continuous line which starts from the critical point of pure CO<sub>2</sub>. As in the binary systems of CO<sub>2</sub> + CO and CO<sub>2</sub> + H<sub>2</sub>, the addition of CO + H<sub>2</sub> results in a decrease in  $T_c$ , but an increase in  $P_c$ ; that is, the slope of the critical curve,  $dP_c/dT_c$  is negative. Also, the absolute value of the slope  $|dP_c/dT_c|$  increases with decreasing ratios of CO:H<sub>2</sub>. This implies that  $P_c$  rises more rapidly compared to the decrease of  $T_c$  when the mixture is richer in H<sub>2</sub>.

## Modeling

The reaction system discussed in this study is a six-component mixture; therefore, it is quite impractical to measure phase diagrams to cover all compositions. Furthermore, apart from critical points, the phase boundary of the reaction mixture needs to be known so that phase separation can be avoided when the reaction conditions are very close to the two-phase region. Therefore, in this section, we use modeling to extend experimental information about the reaction system (e.g., critical

(52) Haselden, G. G.; Newitt, D. M.; Shah, S. M. *Proc. R. Soc. A.* **1951**, *209*, 1-14.

(53) Haselden, G. G.; Snowden, P. *Trans. Faraday Soc.* **1962**, *58*, 1515-1528.

(54) Nagahama, K.; Konishi, H.; Hoshino, D.; Hirata, M. *J. Chem. Eng. Jpn.* **1974**, *7*, 323-328.

(55) Ohgaki, K.; Nakai, S.; Nitta, S.; Katayama, T. *Fluid Phase Equilib.* **1982**, *8*, 113-122.

(56) Kaminishi, G.; Arai, Y.; Saito, S.; Maeda, S. *J. Chem. Eng. Jpn.* **1968**, *1*, 109-116.

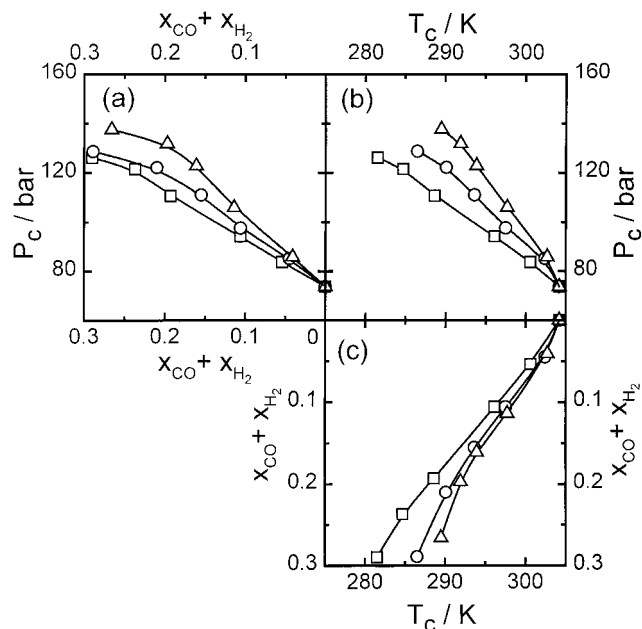


**Figure 5.** The critical points of the ternary system  $\text{CO}_2 + \text{CO} + \text{H}_2$ : (a)  $P$ - $x$  projection, (b)  $P$ - $T$  projection, (c)  $T$ - $x$  projection.  $\Delta$ ,  $\text{CO}:\text{H}_2 = 1:2$ ;  $\circ$ ,  $\text{CO}:\text{H}_2 = 1:1$ ;  $\square$ ,  $\text{CO}:\text{H}_2 = 2:1$ ; —, curves fitted to experimental data.

points) to a comprehensive vapor–liquid equilibrium (VLE) description of the critical region.

We have used the algorithm developed by Heidemann and co-workers<sup>57,58</sup> to calculate the critical points, which is based on the Peng–Robinson equation of state (PR EOS),<sup>59</sup> eq 1. One reason for selecting the PR EOS is that it requires comparatively little input information. For pure substances, only three parameters ( $T_c$ ,  $P_c$ , and the acentric factor) are required to calculate the parameters  $a$  and  $b$ .

$$P = \frac{RT}{v-b} - \frac{a}{v(v+b) + b(v-b)} \quad (1)$$

To extend this equation to mixtures, the van der Waals one-fluid mixing rule is used.  $a$  and  $b$  are calculated from the pure substance parameters by the following equations:

$$a = \sum_i \sum_j x_i x_j (1 - k_{ij})(a_i a_j)^{0.5} \quad (2)$$

$$b = \sum_i x_i b_i \quad (3)$$

where  $x_i$  is the mole fraction of component  $i$ .  $a_i$  and  $b_i$  are the pure substance parameters defined by Peng and Robinson.<sup>59</sup>  $k_{ij}$  represents the binary interaction parameter for the  $i$ - $j$  pair. The literature values<sup>60</sup> for the critical points and acentric factors of the primary components in the reaction mixture are listed in Table 4. The interaction parameters were directly fitted to the experimental critical points of the binary systems when they were available by using an optimization algorithm with the weight factors suggested by Kolár.<sup>61</sup> In other cases, bubble/dew point data for the binary systems were employed to obtain

(57) Heidemann, R. A.; Khalil, A. M. *AIChE J.* **1980**, *26*, 769–779.

(58) Michelsen, M. L.; Heidemann, R. A. *AIChE J.* **1981**, *27*, 521–523.

(59) Peng, D.-Y.; Robinson, D. B. *Ind. Eng. Chem. Fundam.* **1976**, *15*, 59–64.

(60) Reid, R. C.; Prausnitz, J. M.; Poling, B. E. *The Properties of Gases and Liquid*, 4th ed.; McGraw-Hill: New York, 1987.

(61) Kolar, P.; Kojima, K. *Fluid Phase Equilib.* **1996**, *118*, 175–200.

**Table 4.** Pure Component Parameters for Peng–Robinson Equation of State

component	$T_c/\text{K}$	$P_c/\text{bar}$	$\omega$
carbon dioxide <sup>a</sup>	304.1	73.8	0.239
<i>n</i> -butyraldehyde <sup>a</sup>	545.4	53.8	0.352
isobutyraldehyde <sup>a</sup>	513.0	41.5	0.35
propene <sup>a</sup>	364.9	46.0	0.144
carbon monoxide <sup>a</sup>	132.9	35.0	0.066
hydrogen <sup>a</sup>	33.2	13.0	−0.218

<sup>a</sup> Reference 60.

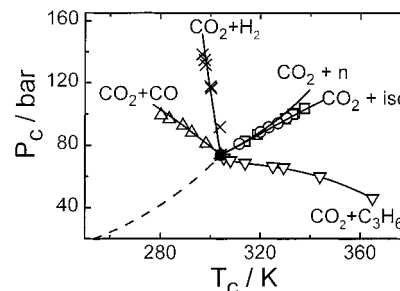


**Figure 6.** Calculated critical loci for binary systems containing  $\text{CO}_2$ :  $\blacksquare$ , critical point of  $\text{CO}_2$ ;  $\square$ , ( $\text{CO}_2 + n$ -butyraldehyde);  $\circ$ , ( $\text{CO}_2 +$  isobutyraldehyde);  $\nabla$ , ( $\text{CO}_2 + \text{C}_3\text{H}_6$ );  $\Delta$ , ( $\text{CO}_2 + \text{CO}$ );  $\times$ , ( $\text{CO}_2 + \text{H}_2$ ); —, curves correlated by PR EOS with the binary interaction parameters given in Table 5; - - -, the vapor pressure curve of pure  $\text{CO}_2$ .

the interaction parameters by minimizing the average absolute deviation in pressure.

**Binary Interaction Parameters.** The six components of our reaction mixture give rise to 15 possible binary mixtures. Therefore, in principle, 15 binary interaction parameters ( $k_{ij}$ ) are required to describe the phase behavior of a six-component system.

Of these 15 mixtures, critical point data for five are reported here, and data for a further mixture have been reported by us previously.<sup>40</sup> VLE data for a further four have been published,<sup>62–65</sup> and the value of  $k_{ij}$  for  $\text{CO}/\text{H}_2$  is already available.<sup>66</sup> Three of the remaining mixtures all involve the *n*- and isobutyraldehydes, and they can be reasonably approximated from the other systems. The final binary is the mixture of the two aldehydes.

The binary critical points measured here have been used to estimate the binary parameters for the systems  $\text{CO}_2 + n$ -butyraldehyde,  $\text{CO}_2 +$  isobutyraldehyde,  $\text{CO}_2 + \text{C}_3\text{H}_6$ ,  $\text{CO}_2 + \text{CO}$ , and  $\text{CO}_2 + \text{H}_2$ . Figure 6 shows the calculated critical curves of these five binary systems, and the average absolute deviations in percent (AAD%) for  $T_c$  and  $P_c$  are listed in Table 6. It can be seen from the Figure and the Table that the correlation correctly reproduces the critical line in the  $\text{CO}_2$ -rich region for each system. The phase behavior of  $\text{CO}_2 + \text{H}_2$  is more complicated than that of the other four systems because of the large size difference between molecules of  $\text{CO}_2$  and  $\text{H}_2$ . Hence, it has previously been found difficult to calculate the critical locus of this binary system with simple mixing rules.<sup>67–69</sup>

(62) Vasil'eva, I. I.; Naumova, A. A.; Polyakov, A. A.; Tyvina, T. N.; Fokina, V. V. *J. Appl. Chem. USSR* **1989**, *62*, 1755–1757.

(63) Vasil'eva, I. I.; Naumova, A. A.; Polyakov, A. A.; Tyvina, T. N.; Fokina, V. V. *J. Appl. Chem. USSR* **1988**, *61*, 404–406.

(64) Polyakov, A. A.; Tyvina, T. N.; Fokina, V. V. *J. Appl. Chem. USSR* **1989**, *62*, 2209–2211.

(65) Williams, R.; Katz, D. L. *Ind. Eng. Chem.* **1954**, *46*, 2512–2520.

(66) Knapp, H.; Döring, R.; Oellrich, L.; Plöcker, U.; Prausnitz, J. M. *Vapor-Liquid Equilibria for Mixtures of Low Boiling Substances*; DECHEMA: Frankfurt/Mn., 1982.

(67) Valderrama, J. O.; Cisternas, L. A.; Vergara, M. E.; Bosse, M. A. *Chem. Eng. Sci.* **1990**, *45*, 49–54.

(68) Huang, H.; Sandler, S. I.; Orbey, H. *Fluid Phase Equilib.* **1994**, *96*, 143–153.



**Table 5.** Binary Interaction Parameters ( $k_{ij}$ ) for Peng–Robinson Equation of State

component $i$	component $j$	$k_{ij}$
CO <sub>2</sub>	<i>n</i> -butyraldehyde	0.101
CO <sub>2</sub>	isobutyraldehyde	0.052
CO <sub>2</sub>	C <sub>3</sub> H <sub>6</sub>	0.067
CO <sub>2</sub>	CO	-0.155
CO <sub>2</sub>	H <sub>2</sub>	0.154 <sup>a</sup>
<i>n</i> -butyraldehyde	isobutyraldehyde	0.0
<i>n</i> -butyraldehyde	C <sub>3</sub> H <sub>6</sub>	0.060 <sup>d</sup>
<i>n</i> -butyraldehyde	CO	0.037 <sup>d</sup>
<i>n</i> -butyraldehyde	H <sub>2</sub>	-1.12642+0.002761T <sup>b,d</sup>
isobutyraldehyde	C <sub>3</sub> H <sub>6</sub>	0.060 <sup>d</sup>
isobutyraldehyde	CO	0.037 <sup>d</sup>
isobutyraldehyde	H <sub>2</sub>	-1.12642+0.002761T <sup>b,d</sup>
C <sub>3</sub> H <sub>6</sub>	CO	-0.191 <sup>d</sup>
C <sub>3</sub> H <sub>6</sub>	H <sub>2</sub>	-0.20748+0.001555T <sup>b,d</sup>
CO	H <sub>2</sub>	0.1 <sup>c,d</sup>

<sup>a</sup> This value of  $k_{ij}$  can only be applied to relatively dilute mixtures H<sub>2</sub> in CO<sub>2</sub> (see text). <sup>b</sup> Binary interaction parameter is temperature dependent.  $T$  is absolute temperature in K. <sup>c</sup> from ref 66. <sup>d</sup> Note that this parameter is set to zero in our final model.

Nevertheless, we tried to fit our experimental data with a single temperature-independent parameter because the mole fraction of H<sub>2</sub> for our data never exceeds 0.21. Gratifyingly, the calculated results showed acceptable deviations for both  $T_c$  and  $P_c$ . However, it must be stressed that this interaction parameter should not be applied to systems with a high mole fraction of H<sub>2</sub>.

For the binary systems, CO<sub>2</sub> + *n*-butyraldehyde and CO<sub>2</sub> + isobutyraldehyde, critical curves were correlated with  $k_{ij}$  equal to 0.102 and 0.052, respectively (see Figure 6), somewhat different from the values obtained by Guo and Akgerman.<sup>70</sup> In their elegant study, temperature-dependent  $k_{ij}$  were fitted to partial molar volume data, 0.11 (45 °C), -0.15 (88 °C) for CO<sub>2</sub>/*n*-butyraldehyde and 0.10 (45 °C), -0.06 (88 °C) for CO<sub>2</sub>/isobutyraldehyde. By contrast, we found no significant improvement in correlating our critical point data (i.e., both  $T_c$  and  $P_c$ ) with temperature-dependent  $k_{ij}$ . Similar fits were obtained for the system CO + C<sub>3</sub>H<sub>6</sub>, the critical points of which have been published previously.<sup>40</sup> The AAD% between calculated and experimental data were 0.2% for  $T_c$  and 3.9% for  $P_c$  (Table 6).

Interaction parameters for four further systems were estimated by fitting literature VLE data. For the systems *n*-butyraldehyde + C<sub>3</sub>H<sub>6</sub><sup>63</sup> and isobutyraldehyde + CO,<sup>64</sup> acceptable fits were obtained with temperature-independent parameters. For the systems *n*-butyraldehyde + H<sub>2</sub><sup>62</sup> and C<sub>3</sub>H<sub>6</sub> + H<sub>2</sub>,<sup>65</sup> the data could only be fitted using temperature-dependent parameters,  $k_{ij} = k_{ij}^a + k_{ij}^b T$ , where  $T$  is the absolute temperature and  $k_{ij}^a$  and  $k_{ij}^b$  are constants. In the absence of literature data for isobutyraldehyde + C<sub>3</sub>H<sub>6</sub> and *n*-butyraldehyde + CO and isobutyraldehyde + H<sub>2</sub>,  $k_{ij}$  were given the same values as for the other isomer.

The interaction parameter for CO/H<sub>2</sub> was set equal to 0.1, the literature value.<sup>66</sup> Finally, because of the similarity of *n*-butyraldehyde and isobutyraldehyde the interaction parameter between them was set to 0. Table 5 summarizes all of the interaction parameters obtained from the binary systems considered in this study.

**Critical Points of Multicomponent Systems.** Our experimentally determined critical points for the multicomponent systems were used as a test of the PR EOS with the obtained

**Table 6.** Average Absolute Deviations in Percent for the Calculated Results of Binary Systems

systems	number of points	AAD%-( $T_c$ ) <sup>a</sup>	AAD%-( $P_c$ ) <sup>b</sup>
CO <sub>2</sub> + <i>n</i> -butyraldehyde	6	0.7	1.8
CO <sub>2</sub> + isobutyraldehyde	5	0.3	1.6
CO <sub>2</sub> + C <sub>3</sub> H <sub>6</sub>	6	0.4	0.6
CO <sub>2</sub> + CO	5	0.5	2.0
CO <sub>2</sub> + H <sub>2</sub>	6	0.1	5.4
CO + C <sub>3</sub> H <sub>6</sub> <sup>c</sup>	5	0.2	3.9

<sup>a</sup> Average absolute deviations in percent for critical temperatures.

<sup>b</sup> Average absolute deviations in percent for critical pressures. <sup>c</sup> Using critical points from ref 40.

interaction parameters. The AAD% between experimental and calculated critical points are given in Table 7. The calculations predict  $T_c$  for 63 experimental points with an average absolute deviation of only 0.3%, while the average absolute deviation for  $P_c$  calculation is 3.0%. The comparison between prediction and experiment is also shown graphically in Figure 7. It is clear that the PR EOS provides good predictions for both  $T_c$  and  $P_c$ , even when the mixtures have six components and large size differences between the molecules. Noticeable scatter only exists in the critical pressure of the two mixtures with high mole fractions of CO + H<sub>2</sub>. It is not easy to judge whether this difference is due to inaccuracies of the model or to experimental error for systems with large amounts of permanent gases.<sup>41</sup>

The PR EOS with 15 parameters is cumbersome. Therefore, we examined the effect of reducing the number of the empirical parameters in the model. For most of the reaction mixtures, the mole fraction of CO<sub>2</sub> is greater than 0.80. Since the mole fractions of C<sub>3</sub>H<sub>6</sub>, CO, H<sub>2</sub>, *n*-, and isobutyraldehyde are all much smaller, these five components could be regarded merely as solutes. Then, the binary interaction parameters between CO<sub>2</sub> and individual solutes would be much more important than those between any two solutes. Therefore, a reduced set of parameters was obtained by setting all of the binary interaction parameters not involving CO<sub>2</sub> to zero and using the values given in Table 5 for the remaining five parameters involving CO<sub>2</sub>. The predictions of the full and reduced sets of parameters were then compared. As might be expected, the differences between the two calculated results increase with  $\chi_0$ , but they are still small. For example, when  $\chi_0 = 0.20$ , the maximum differences are 0.17 K in  $T_c$  and 0.41 bar in  $P_c$ . Indeed, the experimental data are fitted equally well by both sets of parameters. Thus, ignoring  $k_{ij}$  for those pairs without CO<sub>2</sub> does not impair the quality of the model predictions. Therefore, the reduced set (five interaction parameters) was adopted to carry out the remaining calculations.

**CO<sub>2</sub> + CO + H<sub>2</sub>.** The calculated critical points of CO<sub>2</sub> + CO + H<sub>2</sub> are plotted in a  $P$ ,  $T$ ,  $x_{\text{CO}}^{\text{red}}$  phase cube, Figure 8.  $x_{\text{CO}}^{\text{red}}$  is defined as the overall mole fraction of CO on a CO<sub>2</sub>-free basis, as proposed by Kordikowski and Schneider.<sup>71</sup> For comparison, the experimental ternary data and two corresponding binary critical curves are also depicted in Figure 8. The three quasibinary mixtures with  $x_{\text{CO}}^{\text{red}}$  of 0.33, 0.50, and 0.67 can be seen clearly in the phase cube. Although a 3-D figure does not show the deviation between the experimental and calculated values very clearly, it does provide important information about the multicomponent mixture, namely possible pressure maxima or minima in the critical surface. Figure 8 confirms that no pressure maxima or minima occur in the critical surface as the ratio of CO:H<sub>2</sub> is changed.

(69) Ioannidis, S.; Knox, D. E. *Fluid Phase Equilib.* **1999**, *165*, 23–40.  
 (70) Guo, Y.; Akgerman, A. *J. Chem. Eng. Data* **1998**, *43*, 889–892.

(71) Kordikowski, A.; Schneider, G. M. *Fluid Phase Equilib.* **1993**, *90*, 149–162.

**Table 7.** Average Absolute Deviations in Percent for the Calculated Results of Multicomponent Systems

systems	number of components	number of points	AAD%( $T_c$ ) <sup>a</sup>	AAD%( $P_c$ ) <sup>b</sup>
CO <sub>2</sub> + <i>n</i> -butyraldehyde + isobutyraldehyde	3	4	0.6	1.8
CO <sub>2</sub> + CO + H <sub>2</sub>	3	15	0.4	4.5
CO <sub>2</sub> + C <sub>3</sub> H <sub>6</sub> + CO <sup>c</sup>	3	4	0.2	1.6
CO <sub>2</sub> + C <sub>3</sub> H <sub>6</sub> + H <sub>2</sub> <sup>c</sup>	3	2	0.5	4.5
CO <sub>2</sub> + C <sub>3</sub> H <sub>6</sub> + CO + H <sub>2</sub> <sup>c</sup>	4	26	0.2	2.5
CO <sub>2</sub> + <i>n</i> -butyraldehyde + isobutyraldehyde + C <sub>3</sub> H <sub>6</sub> + CO + H <sub>2</sub>	6	12	0.3	2.8
all systems	—	63 <sup>d</sup>	0.3 <sup>e</sup>	3.0 <sup>f</sup>

<sup>a</sup> Average absolute deviations in percent for critical temperatures. <sup>b</sup> Average absolute deviations in percent for critical pressures. <sup>c</sup> Experimental critical points with different ratio of C<sub>3</sub>H<sub>6</sub>:CO:H<sub>2</sub> see ref 43. <sup>d</sup> Total number of the critical points. <sup>e</sup> AAD%( $T_c$ ) for all critical points. <sup>f</sup> AAD%( $P_c$ ) for all critical points.

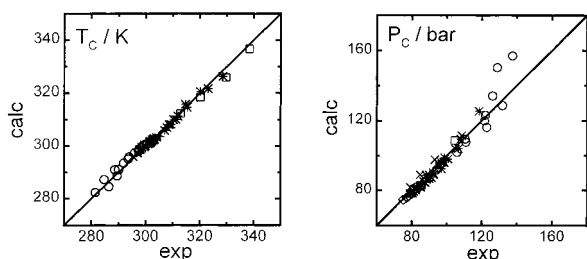


**Figure 7.** Comparison of the experimental and predicted critical points: □, (CO<sub>2</sub> + *n*-butyraldehyde + isobutyraldehyde); ○, (CO<sub>2</sub> + CO + H<sub>2</sub>); ◇, (CO<sub>2</sub> + C<sub>3</sub>H<sub>6</sub> + CO); +, (CO<sub>2</sub> + C<sub>3</sub>H<sub>6</sub> + H<sub>2</sub>); ×, (CO<sub>2</sub> + C<sub>3</sub>H<sub>6</sub> + CO + H<sub>2</sub>); \*, (CO<sub>2</sub> + *n*-butyraldehyde + isobutyraldehyde + C<sub>3</sub>H<sub>6</sub> + CO + H<sub>2</sub>). The solid line is drawn to emphasize that there is a systematic deviation in the calculated values for the system CO<sub>2</sub> + CO + H<sub>2</sub> at higher mole fractions in  $P_c$  calculation of syngas.

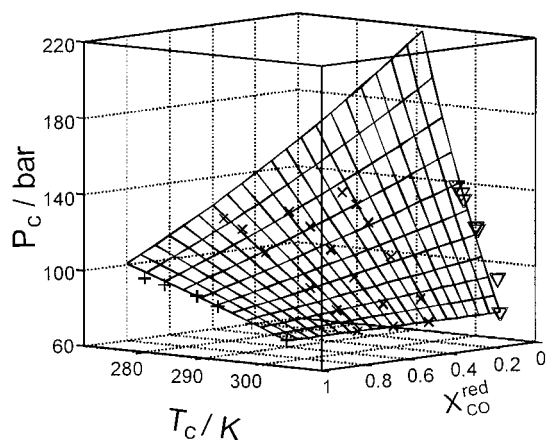


**Figure 8.** Calculated critical points of the ternary system CO<sub>2</sub> + CO + H<sub>2</sub>. The critical surface displayed in a  $P, T, x^{\text{red}}$  phase cube. Experimental critical points are labeled: +, (CO<sub>2</sub> + CO); ∇, (CO<sub>2</sub> + H<sub>2</sub>); ×, (CO<sub>2</sub> + CO + H<sub>2</sub>).

**Six-Component Reaction Mixtures.** Figure 9 shows the predicted critical points of the full six-component reaction mixture as a function of  $\alpha$ , the conversion. The dashed lines indicate mixtures with the same  $\chi_0$ . Although the predicted results from the PR EOS do not coincide exactly with the experimental critical data, the deviations are small, and more importantly, changes in the critical points during the reaction process are simulated correctly. Furthermore, the calculated results show that the PR EOS is capable of predicting the crossover point of the critical temperature with respect to  $\alpha$  (cf. Figure 3a), where  $T_c$  for all mixtures is the same as that of pure CO<sub>2</sub>, 304 K, at  $\alpha = 0.14$ . The model also predicts that there will be a pressure maximum for each reaction mixture but the predicted maximum occur at a somewhat higher conversions,  $\sim +0.2$ , compared to the experimental data.

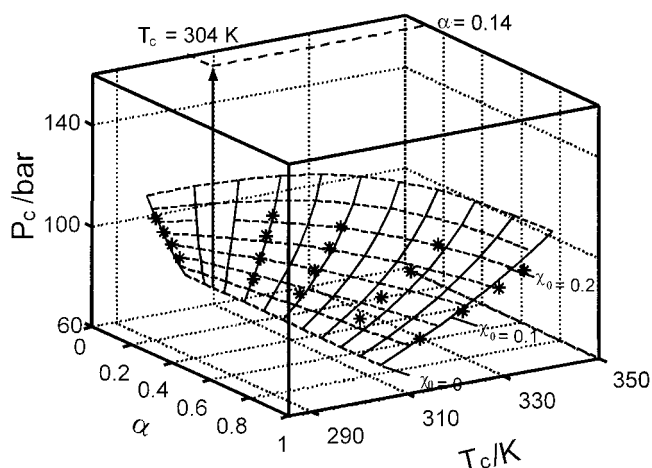


**Figure 9.** Calculated critical points of the six-component reaction mixture. The solid lines indicate the mixture with the same conversion, and the dashed lines link the mixtures of constant  $\chi_0$ . \*, experimental critical points taken from Figure 3.

**Controlling the Phase Behavior of Reaction Mixtures. (a) Keeping a Reaction Mixture in a Single Phase.** The previous sections have shown that the critical temperatures and pressures of the reaction mixtures change substantially during the reaction. Here we consider how a mixture can be kept in a single phase throughout the reaction. The problem is that a mixture can separate into two phases at temperatures and pressures other than  $T_c$  and  $P_c$  by crossing the vapor/liquid-phase boundary. We begin by using our model to calculate how the phase boundary changes during the reaction.

An efficient procedure described by Michelsen<sup>72</sup> was used to construct the phase boundary ( $P$  versus  $T$  at a fixed composition). The mole ratio of C<sub>3</sub>H<sub>6</sub>:CO:H<sub>2</sub> and of two butyraldehydes were kept at 1:1:1 and 8:1, respectively, and  $\chi_0$  was fixed at 0.20. Figure 10a presents the calculated phase boundaries for a number of mixtures with  $\alpha$  ranging from 0 to 1. The calculated and experimental critical points of the mixtures are shown as the solid and open points, respectively. For the mixture CO<sub>2</sub> + C<sub>3</sub>H<sub>6</sub> + CO + H<sub>2</sub> (i.e.,  $\alpha = 0$ ), the critical point is located at the head of the  $P$ - $T$  loop, and it is close to the point of maximum temperature. However, the critical point for mixtures with large  $\alpha$  are located far below the temperature maximum. It should be noticed that the critical point is neither the point of maximum pressure, nor that of maximum temperature in the  $P$ - $T$  phase diagram (Figure 10a). In fact, at  $\alpha = 1$ , the location of the critical point means that there is a large area of  $P, T$  space in which retrograde condensation can occur.

**(b) Continuous Reactions.** We now consider how the reaction mixture can be kept as a single phase throughout the reaction (i.e., from  $\alpha = 0$  to  $\alpha = 1$ ). We begin by considering

(72) Michelsen, M. L. *Fluid Phase Equilib.* **1980**, *4*, 1–2.



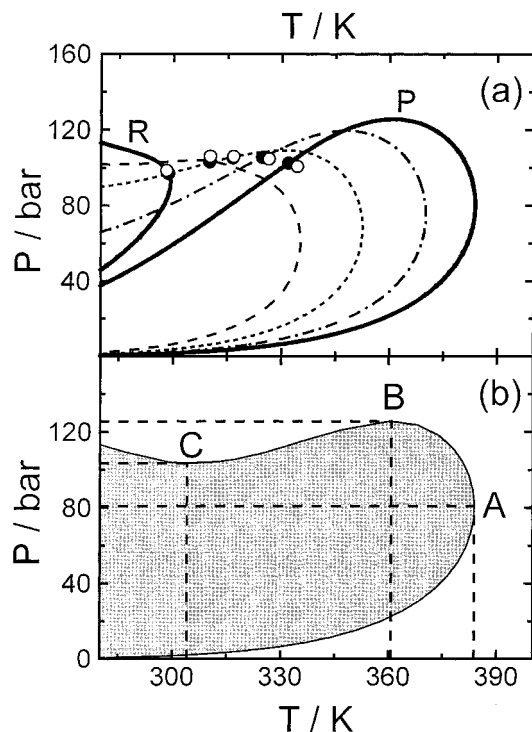


**Figure 10.** Calculated phase boundary for the six-component reaction mixture: the initial total mole fraction is 0.20, and the molar ratio C<sub>3</sub>H<sub>6</sub>:CO:H<sub>2</sub> and *n*-butyraldehyde:isobutyraldehyde is 1:1:1 and 8:1. (a) Phase boundary at different conversion: — R,  $\alpha = 0$ ; - - -,  $\alpha = 0.30$ ; ···,  $\alpha = 0.49$ ; - · - ·,  $\alpha = 0.75$ ; — P,  $\alpha = 1.00$ . Solid symbols ●, represent the calculated critical points, which lie on the calculated phase boundary under each conversion. Open symbols ○, represent experimental critical points for the corresponding conversion. (b) The envelope of the global two-phase region during the reaction.

a reaction carried out under conditions of constant pressure as, for example, in a flow reactor. To do this we construct an unusual type of phase diagram by drawing the overall envelope of all the two-phase regions in Figure 10a to give the curve in Figure 10b. The gray region of Figure 10b now represents the area of *P, T* space in which a reaction mixture will be two-phase at some moment during the reaction.

Three points have been highlighted in Figure 10b. Point A is a temperature maximum 384 K, above which the reaction mixture will always be a single phase irrespective of the pressure. Point B is a pressure maximum, 126 bar, above which the mixture will be single phase at any temperature above 280 K (the lower-temperature limit of this Figure). Of course, in both cases, the single phase will not necessarily be “supercritical”, in that the density could be much lower (or higher) than the critical density of the mixtures. The third point C (304 K, 104 bar) is particularly interesting because it shows the lowest pressure which can be used at any temperature below 304 K. However, if the temperature is either higher or lower than 384 K, the mixture will enter two phases at some point in the reaction. It must be stressed that all of these conclusions apply to just one initial mole fraction of reactants, 0.2. However, a similar analysis could obviously be applied to other concentrations.

This analysis has considered a reaction being carried out under constant pressure. However, the reaction consumes CO and H<sub>2</sub>, both of which make major contributions to the pressure of the system. Thus, pressure can only be maintained if the density of the system rises as the reaction proceeds. Figure 11 indicates how the density  $\rho$  increases as a function of  $\alpha$  for reactions run at three different pressures at 361 K. In each case,  $\rho$  increases

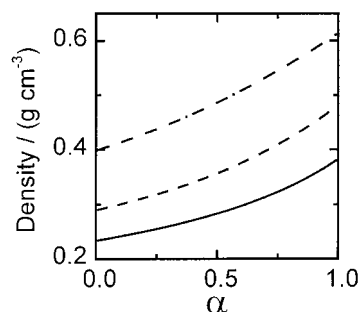


**Figure 11.** Density dependency<sup>73</sup> on conversion at 361 K: the initial total mole fraction is 0.20, and the molar ratio C<sub>3</sub>H<sub>6</sub>:CO:H<sub>2</sub> and *n*-butyraldehyde:isobutyraldehyde is 1:1:1 and 8:1. —, 126 bar; - - -, 150 bar; ···, 200 bar. The dotted horizontal line at  $\rho = 0.38 \text{ g cm}^{-3}$  indicated the change in pressure needed to keep a mixture in a single phase in a sealed batch reaction at 361 K with a final pressure of 126 bar.

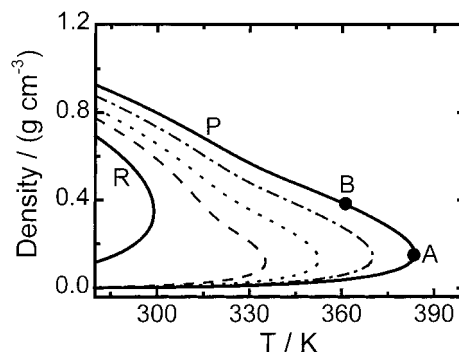


**Figure 12.** Density<sup>73</sup> at the phase boundaries shown in Figure 10: — R,  $\alpha = 0$ ; - - -,  $\alpha = 0.30$ ; ···,  $\alpha = 0.49$ ; - · - ·,  $\alpha = 0.75$ ; — P,  $\alpha = 1.00$ .<sup>74,75</sup>

by ~50% in the course of the reaction. This implies that, for a reaction run in a tubular flow-reaction, the density of the mixture will increase substantially along the length of the reactor with a corresponding reduction in linear velocity of the mixture through the reactor.

**(c) Reactions under Batch Conditions.** The majority of SCF reactions, including most of the published studies on the hydroformylation of C<sub>3</sub>H<sub>6</sub>, are currently run as batch processes in a sealed autoclave. This means that the pressure cannot be held constant in a reaction such as this where a gas (or gases) are consumed. Instead, batch reactions are run under conditions of constant density,  $\rho$ . Figure 10a can only be applied to batch reactions, if  $T > 384 \text{ K}$ , where the reaction mixture is the single-phase irrespective of pressure. For lower temperatures, one needs to consider a quite different diagram, Figure 12, involving  $\rho$  and *T*.

Figure 12 shows the  $\rho$ -*T* phase boundary for the same reaction mixture as that used to construct the *P*-*T* phase boundary in Figure 10 over the same range of  $\alpha$ . For a given value of  $\alpha$ , the mixture will split into two phases when overall density and temperature are located inside the phase boundary. Again, the point A indicates the temperature maximum, 384 K, above which the reaction mixture will be homogeneous irrespective of density.

Unlike the *P*-*T* boundaries (Figure 10a), the  $\rho$ -*T* boundaries for the mixtures with different  $\alpha$  do not intersect in the critical region. The size of the  $\rho$ -*T* loops increases with  $\alpha$ . This implies that the reaction mixture will always be homogeneous as the reaction proceeds if the overall density and temperature are outside the two phases region for the final mixture with  $\alpha = 1$ . Thus, at any given temperature, the overall density for the

mixture with  $\alpha = 0$  must be high enough to ensure that it exceeds the density needed to make the final mixture ( $\alpha = 1$ ) single phase at that temperature. This is not an easy condition to satisfy because the pressure needed to the required density for  $\alpha = 0$  may be quite high. For example, at 361 K, the density at the phase boundary is  $0.38 \text{ g cm}^{-3}$  for the mixture with  $\alpha = 1$ , and an initial pressure  $>200$  bar is needed to achieve this (see Figure 11). By contrast, Figure 10b shows that only 126 bar is needed to keep the reaction mixture in a single phase under conditions of constant pressure as in a flow reactor at this temperature (point B).

Therefore, at a given temperature, a batch reactor may need to be run under much higher pressures than a flow reactor if single-phase conditions are to be preserved throughout the course of the reaction. This conclusion assumes that no more syngas is added as the reaction proceeds. Such an addition might well be a useful strategy on chemical grounds, but addition of CO and H<sub>2</sub> will probably reduce the miscibility of the system even further.

### Conclusions

This paper has presented for the first time data showing how the critical point of a reaction mixture changes as the reaction proceeds from reactant to product. It has also shown how these data can be used to validate the modeling of the phase behavior and to draw overall conclusions about strategies for controlling the phase separation of the reaction mixture.

Once the initial concentrations of the reactants have been fixed, the stoichiometry of the reaction will define all of the concentrations at subsequent stages of the reaction. Therefore, irrespective of the number of components, the overall behavior can be described by only two parameters, the initial mole fraction and the degree of conversion.

Any study of this type requires some simplification, and in our case we have considered a relatively simple reaction, the hydroformylation of C<sub>3</sub>H<sub>6</sub>, and have studied only a narrow range of compositions. Nevertheless, we believe that our main conclusions will have much wider applicability. In particular, we have shown:

(1) In multicomponent reaction mixtures, the concentration of any individual components will be low in most experimental situations. Therefore, binary interactions between pairs of components apart from those involving the SCF solvent, can be ignored without introducing significant errors. Thus, models of the phase behavior will only require a relatively small number of parameters.

(2) We have introduced a new type of phase envelope, see Figure 10b, which defines the boundary inside which a reaction mixture will separate into gas and liquid phases at some point during the reaction.

(3) We have shown that different experimental strategies may be needed to keep a mixture in one phase in batch reactors and in continuous reactors. In general, for reactions such as this one involving permanent gases, a significantly higher initial pressure may be needed for batch reactions.

(4) We have demonstrated that acoustic techniques can provide a major body of data on critical points in a reasonable length of time. These measurements have agreed well with more conventional measurements in view cells but are considerably less time-consuming.

We hope that our results will encourage others to tackle the problems of the phase behavior of reaction mixtures because we believe that control of phase behavior is one of the keys to controlling chemical reactions in supercritical fluids. Currently, we are extending the work to the hydrogenation of propene.<sup>76</sup>

**Acknowledgment.** We thank Dr. A. Cabañas, Dr. P. J. King, Dr. C. J. Mellor, Mr. R. M. Oag, Mr. C. Valder, Mr. D. Merrifield and Professor J. F. Brennecke for their help and advice. We thank Mr. M. Guylar and Mr. K. Stanley for their technical assistance. We are grateful to EPSRC, GlaxoSmith-Kline Plc, and the Royal Society for financial support and acknowledge support from National Natural Science Foundation of China, Office of Science and Technology of UK, and Ministry of Science and Technology of China.

**Note Added in Proof.** A very recent paper addresses the phase separation of an eight-component mixture for allylic oxidation in supercritical CO<sub>2</sub>: Stradi, B. A.; Stradtherr, M. A.; Brennecke, J. F. *J. Supercrit. Fluids* **2001**. In press.

JA003446O

(73) The calculated density in Figure 12 is based on the liquid density at the bubble point and the vapor density at the dew point, and those shown in Figure 11 are the calculated density in a single-phase region. It is likely that the results are only semiquantitative because cubic equations of state are known to give rather poor predictions of density, especially in the critical region.<sup>74,75</sup> However, we believe that the calculation describes the changes of  $\rho$ - $T$  boundary sufficiently well for the purposes of our discussion.

(74) Chou, G. F.; Prausnitz, J. M. *AIChE J.* **1989**, *35*, 1487–1496.

(75) Kutney, M. C.; Dodd, V. S.; Smith, K. A.; Herzog, H. J.; Tester, J. W. *Fluid Phase Equilib.* **1997**, *128*, 149–172.

(76) Ke, J.; Han, B.; George, M. W.; Yan, H.; Poliakoff, M. *J. Phys. Chem.* Manuscript to be submitted.